

## Poly(anthranilic acid) Microspheres: Synthesis, Characterization and their Electrocatalytic Properties

Suresh Ranganathan, Prabu Raju, Vijayaraj Arunachalam, Giribabu Krishnamoorthy, Manigandan Ramadoss, Stephen Arumainathan,<sup>†</sup> and Narayanan Vengidusamy\*

Department of Inorganic Chemistry, University of Madras, Guindy Maraimalai Campus, Chennai 600025, India

\*E-mail: vnmara@yahoo.co.in

<sup>†</sup>Department of Nuclear Physics, University of Madras, Guindy Maraimalai Campus, Chennai 600025, India

Received January 12, 2012, Accepted March 12, 2012

Poly(anthranilic acid) was synthesized by rapid mixing method using 5-sulphosalicylic acid as a dopant. The synthesized polymer was characterized by various techniques like FT-IR, UV-Visible, and X-ray diffraction *etc.*, The FT-IR studies reveal that the 5-sulphosalicylic acid is well doped within the polymer. The morphological property was characterized by field emission scanning electron microscopic technique. The electrochemical properties of the polymer were studied by cyclic voltammetric method. The synthesized polymer was used to modify glassy carbon electrode (GCE) and the modified electrode was found to exhibit electrocatalytic activity for the oxidation of uric acid (UA).

**Key Words :** Conducting polymer, Sulphosalicylic acid, Uric acid, Electrocatalyst, Modified electrode

### Introduction

The conducting polymers have emerged as a new class of materials because of their unique electrical, optical and chemical properties. Among them, PANI has been the most studied polymer owing to its high conductivity, environmental stability and low cost of production. It has potential application in areas such as sensors,<sup>1-4</sup> gas separation membranes,<sup>5</sup> light emitting diodes,<sup>6-8</sup> electrochromic and electronic devices,<sup>9-11</sup> and as cathode materials in lithium batteries<sup>12</sup> *etc.*, It can be synthesized conveniently either as a powder or as a film by chemical and electrochemical routes.<sup>13,14</sup> However one drawback of PANI is its poor processability. PANI itself is not soluble in aqueous and most non-aqueous solvents and it decomposes before it melts. In order to improve its processability a few authors have reported on the complexation of PANI with sulphonic acids.<sup>15</sup> Alternative way is to use derivatives of PANI like poly(methylaniline),<sup>16</sup> poly(2-methoxyaniline),<sup>17</sup> poly(2-aminophenol)<sup>18</sup> and poly(2-anthranilic acid)<sup>19</sup> *etc.*, It is believed that the substituent in polymer chain decrease the stiffness of the polymer making it easier to dissolve.<sup>20</sup> In this view, anthranilic acid is an important monomer for the synthesis of carboxylic acid group substituted PANI. Similar to the poly(methanilic acid),<sup>21</sup> it is expected that poly(anthranilic acid), PANA, possesses electrochemical activity over a wide pH range in aqueous solutions due to the substitution of carboxylic acid group. However, the PANA (with or without external dopant HCl) exhibit very low conductivity compared to PANI.<sup>22</sup> Also, studies on the synthesis of PANA from acidic aqueous solutions are rarely reported in the literature, probably due to its high solubility. It is well known that by using proper dopant, changes the electrical conductivity of the non-conducting or very low

conducting polymer to a semiconducting or metallic conducting polymer. For instance, Entezami *et al.*<sup>23</sup> have reported that the conductivity of SSA doped PANI is several magnitude higher than that of PANI.

In this paper, we have reported the synthesis of 5-sulphosalicylic acid doped poly(anthranilic acid) (PANA-SSA) microspheres and characterized its structural, optical, and electrochemical properties. Additionally we have performed the electrocatalytic activity of the synthesized PANA-SSA towards the oxidation of UA. Hence the PANA-SSA has been used to modify the GCE and remarkable enhancement in the current response with shift in anodic peak potential is observed for electrochemical oxidation of UA when compared to the bare electrode.

### Experimental

**Materials.** Anthranilic acid, potassium persulfate, 5-sulphosalicylic acid, sodium dihydrogen phosphate and disodium hydrogen phosphate were purchased from Qualigens and used without further purification. Uric acid was purchased from Sigma and used as received. Doubly distilled water was used as the solvent.

**Synthesis of Poly(anthranilic acid).** In a typical synthesis, 0.69 g (5 mmol) of anthranilic acid and 1.27 g (5 mmol) of sulphosalicylic acid were dissolved in required amount of double distilled water. The solution was cooled at 5 °C for 30 min and then a pre-cooled aqueous solution of potassium persulfate as an oxidant were rapidly added. The molar ratio of oxidant to anthranilic acid in the final solution was 1:1. The reaction continued for 16 h during which the precipitation of black colored poly(anthranilic acid) was observed. The obtained poly(anthranilic acid) was filtered and dried in vacuum at room temperature for 48 h.

**Characterization Methods.** FT-IR spectrum of the polymer was recorded on Shimadzu FT-IR 8300 series instrument by using potassium bromide pellet. The UV-Visible spectrum of polymer was recorded on UV-1601OC, Shimadzu instrument using absolute ethanol as solvent. The electrochemical experiments were performed on a CHI 600A electrochemical instrument using the as-modified electrode and bare GCE as working electrode, a platinum wire was the counter electrode, and saturated calomel electrode (SCE) was the reference electrode. The nature of the sample was determined by using Rich Siefert 3000 diffractometer with monochromatic  $\text{Cu K}\alpha_1$  radiation ( $\lambda = 1.5406 \text{ \AA}$ ). The morphology of the polymer was analyzed by FE-SEM using a HITACHI SU6600 field emission-scanning electron microscopy.

**Preparation of PANA-SSA Modified GCE is as Follows.** Ultrasonic agitation for 30 min was used to disperse 1 mg of PANA-SSA into 5 mL of water to make blackish brown suspension. 10  $\mu\text{L}$  of the PANA-SSA suspension was mixed with 10  $\mu\text{L}$  of 5% nafion. 5  $\mu\text{L}$  of the nafion mixed suspension was coated on the polished GCE and dried at room temperature.

## Results and Discussion

**Structure and Morphology.** Figure 1 represents the FTIR spectrum of PANA-SSA which is in good agreement with previously reported spectrum for PANA.<sup>24</sup> The band assignments for PANA-SSA are given in Table 1. The peak at 1566 and 1511  $\text{cm}^{-1}$  correspond to the C=C stretching deformation of quinoid and benzenoid rings respectively. The peak at 1686  $\text{cm}^{-1}$  is due to stretching vibration of C=O of -COOH group. The peak at 1317  $\text{cm}^{-1}$  is assigned to the C-N stretching of the secondary aromatic amine group. The peak observed at 756 and 593  $\text{cm}^{-1}$  are assigned to C-H out-of-plane bending vibrations of benzene nuclei in the polymer chain. The peak at 1250  $\text{cm}^{-1}$  is commonly attributed to the C-N<sup>+</sup> stretching vibration in the polaron structure, indicating that the PANA is in the doped state.<sup>25</sup> In addition to these

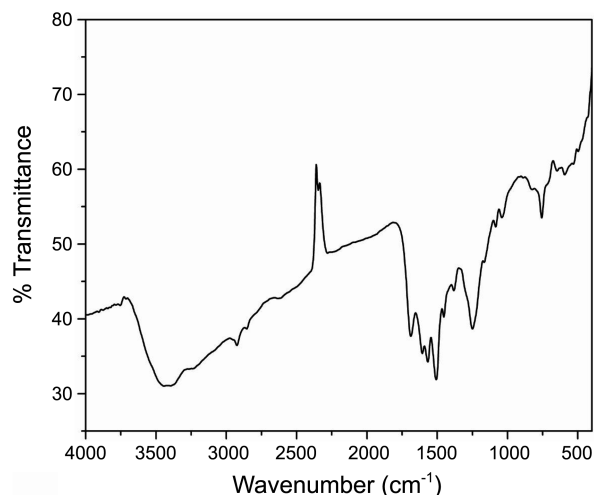


Figure 1. FT-IR spectrum of PANA-SSA.

Table 1. FT-IR Band assignments of the PANA-SSA

Stretching vibration ( $\text{cm}^{-1}$ )	Band assignment
1566	C=C stretching deformation of quinoid ring
1511	C=C stretching deformation of benzenoid ring
1317	C-N stretching of secondary amine
1250	C-N <sup>+</sup> stretching vibration
1686	C=O stretching vibration of carboxylic group
1141 to 1021	Asymmetric and symmetric stretching vibration of O=S=O
800 to 600	Stretching mode of C-S and S-O group
756 and 593 $\text{cm}^{-1}$	C-H out-of-plane bending vibrations of benzene nuclei

peaks, the peak at 1141, 1021, and 800-600  $\text{cm}^{-1}$ <sup>26</sup> are due to the SSA. The presence of these peaks clearly confirms that SSA is incorporated within the PANA.

The UV-Visible spectrum of PANA-SSA is shown in Figure 2. The solution spectrum of PANA-SSA shows the peak at 532 and 361 nm. The peak observed at 532 nm corresponds to exciton like transition in quinoid diimino units. The another peak that appear at 361 nm is attributed to  $\pi$ - $\pi^*$  transition in benzenoid unit which relates to the extent of conjugation between adjacent phenyl groups in the polymer chain. Compared with the same characteristic absorption peak of EB-PANI, it shifts to the longer wavelength (red shift), which indicates that the conjugate conjunction of PANA-SSA decreased compared with EB-PANI. It may be due to the resistance effect of -COOH groups which decreases the planar conjugate conjunction of the aromatic rings and -COOH groups present in the backbone of the polymer chain are strongly attracting an electron radical which decreases the electron cloud density of aromatic rings.<sup>27</sup>

The XRD pattern of SSA doped PANA is shown in Figure 3, which proves the amorphous character of the synthesized polymer. The broad peak centered at  $2\theta = 25^\circ$  may be ascribed to the periodicity perpendicular to the polymer chain.<sup>28</sup>

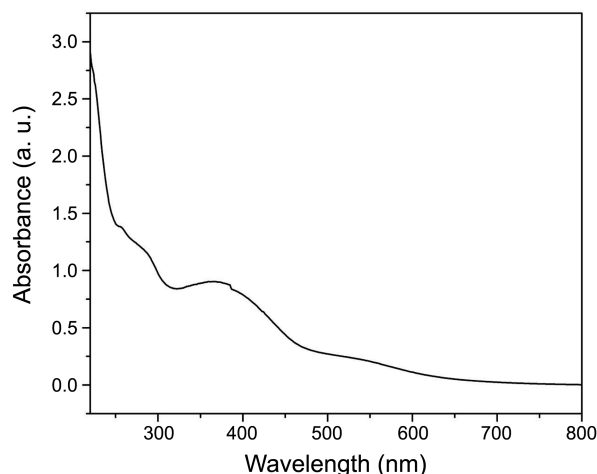


Figure 2. UV-Visible spectrum of PANA-SSA.

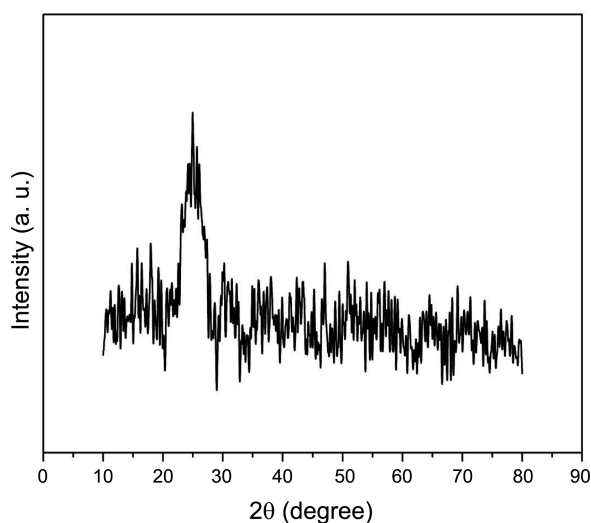


Figure 3. XRD pattern of PANA-SSA.

The morphology of the PANA-SSA was studied by FE-SEM which is shown in Figure 4. From the FE-SEM image (Figure 4(a)), it is clear that the synthesized PANA-SSA is sphere shaped particles with voids. The size of the microsphere is in the range of 1 to 5  $\mu\text{m}$ . The expanded image of single microsphere (inset in Figure 4(a)) reveals that there is oval shaped void present at the top of the microsphere. The formation mechanism of PANA-SSA microsphere is as follows: Anthranilic acid formed micelle droplets in aqueous solution in the presence of SSA, which act as templates for the polymerization. The micelle droplets were formed due to the presence of a hydrophilic  $-\text{NH}_2$  and  $-\text{COOH}$  groups and hydrophobic  $-\text{C}_6\text{H}_4$  group. When the addition of an oxidant, which is hydrophilic, the polymerization took place at the interface of water/droplet to produce small spherical nanostructures.<sup>29</sup> It is well known that the oxidative polymerization of aniline and its derivative is an exothermic process.<sup>30</sup> Hence the heat released during the oxidation of anthranilic acid will increase the local temperature of droplets, which results in the fusion of droplets to form the larger microspheres. It can be clearly seen from Figure 4(a) that there are voids on the surface of PANA-SSA microspheres which is due to the diffusion of monomers to outside.<sup>29</sup> Figure 4(a) also displays there some broken microspheres which showed that the microsphere is not a hollow one. Further magnification images of these broken microspheres reveal that the microsphere is constructed by the nanoparticles (Figure 4(b) and (c)).

**Electrochemical Property.** The electrochemical behavior of PANA-SSA on GCE was tested through cyclic voltammetric measurements in an acidic electrolyte. Figure 5 depicts the oxidation/ reduction process of PANA-SSA on GCE. Unlike polyaniline and many of its substituted forms, generally PANA does not show well-defined redox peaks due to its non conducting nature. However PANA-SSA shows broad peaks in the potential range from 1 to 0.8 V. Hence the synthesized PANA-SSA is an electroactive polymer which may be due to the dopant, SSA. Figure 5 shows a

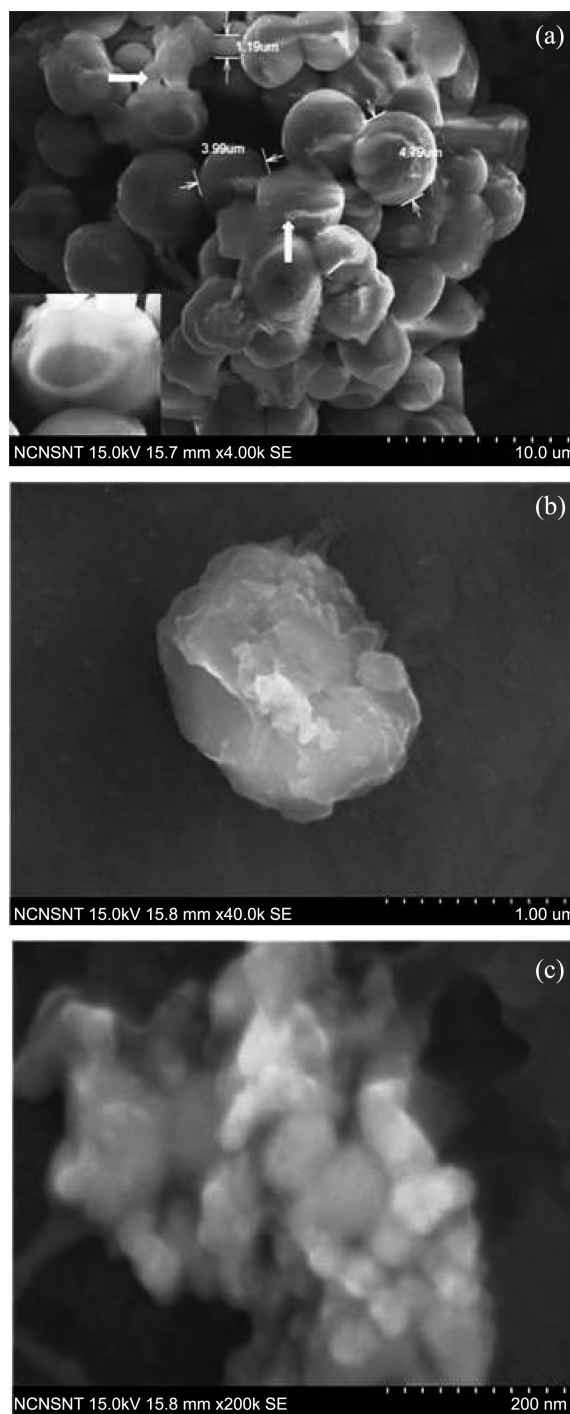
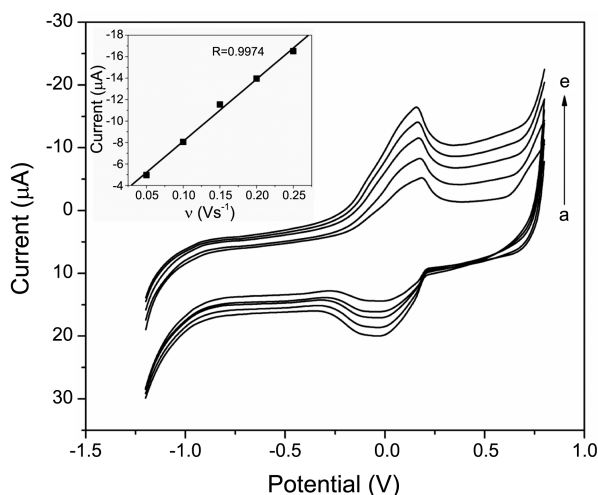


Figure 4. FE-SEM images of PANA-SSA (a) lower magnification, (b) and (c) higher magnification.

pair of peaks at 0.209 V/0.03 V, which are corresponding to emeraldine/pernigraniline reversible transition. Different scanning rates were used to examine the dynamic property of PANA-SSA during the redox process. As is shown in Figure 5, the peak current is directly proportional to the scan rates with a calibration equation of  $I(\mu\text{A}) = (2.3175) + 57.934v$  ( $\text{Vs}^{-1}$ ) ( $r = 0.99744$ ), suggesting an electric charge-transfer controlled process (inset in Figure 5). The surface coverage ( $\Gamma$ ) was evaluated from the area under the anodic



**Figure 5.** Cyclic voltammogram of PANA-SSA modified GCE at a scan rate of (a) 50, (b) 100, (c) 150, (d) 200 and (e) 250  $\text{mV s}^{-1}$ . Inset Figure: Anodic peak current vs scan rate.

peak of the cyclic voltammograms for the PANA-SSA modified GCE. According to Laviron's equation,<sup>31</sup> the surface coverage of the electrode can be calculated by using the following equation,

$$\Gamma = Q/nFA$$

where  $n$  represents the number of electrons involved in the redox process ( $n = 2$ ),  $A$  is the surface area of the electrode ( $0.0707 \text{ cm}^2$ ) and  $\Gamma$  represents the surface coverage concentration ( $\text{mol cm}^{-2}$ ). From the above, the calculated surface coverage of PANA-SSA layer was  $2.22 \times 10^{-9} \text{ mol cm}^{-2}$ .

**Electrocatalytic Property.** Figure 6 shows the cyclic voltammogram (CV) of 0.5 mM UA at bare and PANA-SSA modified GCE. The CV of UA (curve a) at the bare GCE shows a peak at about 0.54 V as previously reported by Yang *et al.*<sup>32</sup> It is well known that the oxidation of UA at bare GCE is generally believed to be totally irreversible and requires high over potential. However the UA voltammogram obtained for PANA-SSA modified GCE showed an

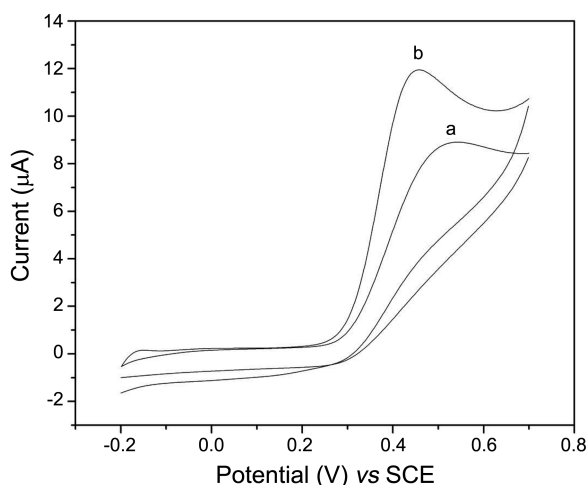
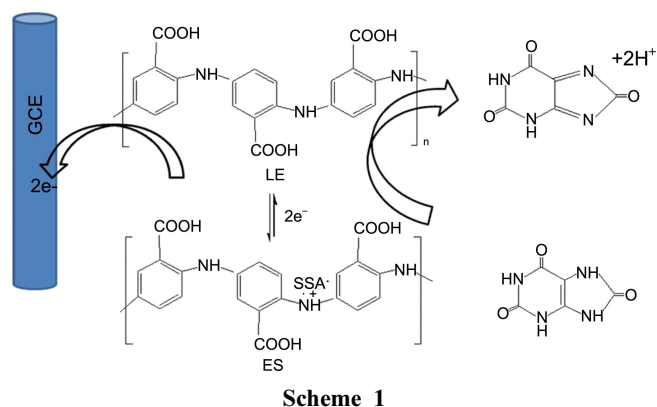


**Figure 6.** Cyclic voltammogram of 0.5 mM UA on PANA-SSA modified GCE at 50  $\text{mV s}^{-1}$ .



oxidation wave with a potential range at 0.46 V with enhanced peak current than the bare GCE. Hence, the PANA-SSA modified electrode has improved the electron transfer kinetics. The anodic peak potential is shifted to the negative direction by 80 mV indicates the electrocatalytic ability of the modified electrode. It is reported that the oxidation of UA is irreversible at GCE and the oxidation of UA proceeds *via*  $2e^-$ ,  $2H^+$  process.<sup>32</sup> According to the previous reports,<sup>32,33</sup> the detailed electrochemical oxidation mechanism of UA at PANA-SSA modified GCE can be explained by the Scheme 1.

Figure 7 shows the effect of scan rate on PANA-SSA modified GC electrode in 0.5 mM UA. The slight shift towards higher values of the oxidation peak potential with increasing scan rates can be observed, indicating a kinetic limitation in the reaction between redox sites of PANA-SSA modified GC electrode and UA. However, the anodic peak currents for UA at PANA-SSA modified GC electrode are linearly related to the scan rate in the range of 25-250  $\text{mV s}^{-1}$  with a calibration equation of  $I(\mu\text{A}) = 8.5886 + 19.6v (\text{Vs}^{-1})$  ( $r = 0.9843$ ), which indicated that the electron transfer reaction was controlled by adsorption process. In order to determine the adsorption behaviour of UA, we have

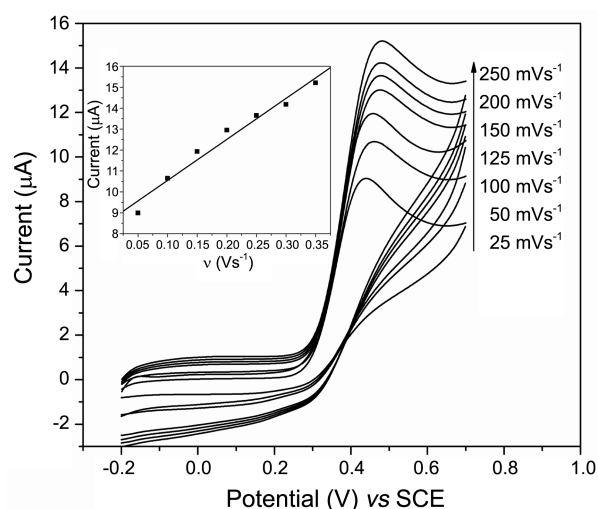


**Figure 7.** Cyclic voltammogram of 0.5 mM UA on PANA-SSA modified GCE at different scan rates. Inset Figure: Plot of anodic peak current vs. scan rate.

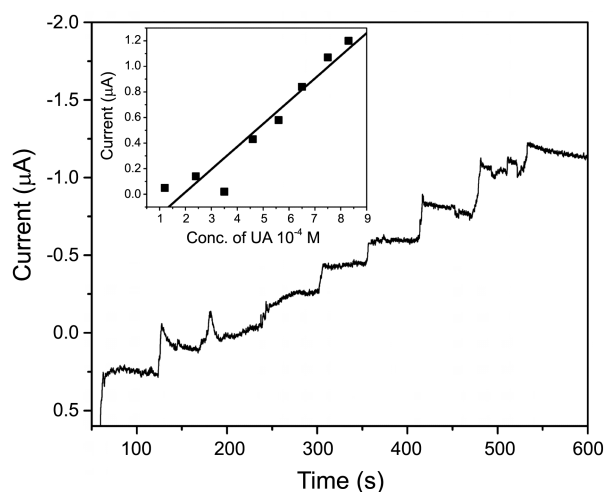


**Figure 8.** Chronoamperometric response of PANA-SSA modified GCE. Inset Figure: Plots of anodic peak current vs. the concentration of UA.

performed the following experiment. After the PANA-SSA modified GCE was used for the determination of UA, it was transferred to the blank supporting electrolyte, there was a voltammetric signal for the oxidation of UA appeared, and confirming that UA was adsorbed at the PANA-SSA modified GCE during oxidation process. Chang *et al.*<sup>34</sup> reported that the UA can form hydrogen bonding with oxo-surface groups, especially -COOH group in graphene oxide. This adsorption property eliminates the determination of UA from interfering species like ascorbic acid. In our case, the adsorption of UA at the modified electrode may be due to the presence of -COOH group in the PANA-SSA. The relation between the anodic peak potential and  $\log v$  was constructed. From the plot of  $E_{pa}$  vs  $\log v$ , the calculated slope is 0.046. According to Laviron equation, the  $E_{pa}$  for an adsorption controlled and irreversible electrode process is defined by the following equation:

$$E_{pa} = E^{\circ} + \frac{RT}{\alpha nF} 2.303 \log(RT k^{\circ} / \alpha nF) + 2.303 \frac{RT}{\alpha nF} \log v$$

Hence the value of  $\alpha n$  can be calculated from the slope of the linear plot of  $E_{pa}$  vs  $\log v$ . Generally,  $\alpha$  is assumed to be 0.5<sup>35</sup> for totally irreversible electrode process. Therefore, the number of electron ( $n$ ) transferred in the electrochemical oxidation of UA is 2.5. The findings are consistent with that mentioned earlier, on the oxidation of UA mechanism.

**Table 2.** Comparison of PANA-SSA modified GCE with other modified electrodes

Sensor	Ref. electrode	pH	Anodic potential (V)	References
PPy NEEs/GCE	SCE	7.4	0.60	[32]
Pd/TiO <sub>2</sub> /CHIT/GCE	SCE	7.4	0.50	[36]
L-Cys/Au electrode	SCE	4.6	0.47	[33]
Pt-Fe(III)/DNA/GCE	SCE	5.0	0.43	[37]
PANA-SSA/GCE	SCE	7.4	0.45	This work

On the basis of the voltammetric results described above, it appears likely that chronoamperometric detection of uric acid by the PANA-SSA modified GCE is possible. According to the potential dependence of the uric acid electrocatalytic oxidation current at stirring conditions, the optimum electrode potential was selected at 0.5 V versus SCE for chronoamperometric measurements in order to obtain repeatability and sensitivity. Figure 8(a) displays the chronoamperometric response of the PANA-SSA modified GC electrode upon the addition of 1 mL of 0.1 mM UA. A successive addition of UA to continuously stirred 0.1 M PBS produces a significant increase in the current. The calibration plot of the PANA-SSA modified GC electrode is shown as inset in Figure 8. The linear chronoamperometric response is in the range from  $1 \times 10^{-4} \sim 9 \times 10^{-4}$  M corresponding with a sensitivity of 0.18  $\mu\text{A}/\text{mM}$ , shows that the PANA-SSA modified GC electrode is sensitive towards the UA.

The storage stability of the PANA-SSA modified GCE was investigated for the consecutive 30 days. The response to the oxidation of the same concentration of UA at the optimum oxidation potential was maintained at 93% of the initial values. The long term stability of the PANA-SSA modified GCE could be attributed to the structure stability and the easy preparation method of the sensor. The PANA-SSA modified GCE is compared with other electrode materials (Table 2).<sup>36,37</sup> The developed modified electrode has the comparable results over the others in the list as it has produced lowest anodic peak potential.

## Conclusions

The SSA doped PANA nanoparticles were synthesized by rapid mixing method. The FTIR spectrum confirms the formation of PANA-SSA. It also confirms that SSA is incorporated within the PANA nanoparticles. UV-Visible spectrum showed the presence of -COOH group in aromatic ring of aniline which produces red shift. Cyclic voltammogram shows that the PANA-SSA nanoparticles have electrochemical activity. At pH 7.4 PBS, PANA-SSA modified GCE exhibits good electrochemical activity for the oxidation of UA. The modified electrode prepared is very stable and can be utilized for the quantitative determination of UA.

**Acknowledgments.** One of the author (RS) acknowledges the University of Madras for the financial assistance in the form of Dr Kalaingar M. Karunanidhi Endowment Scholarship. We acknowledge the FE-SEM facility provided by the National Centre for Nanoscience and Nanotechnology, University of Madras.

## References

- Li, M.; Guo, Y.; Wei, Y.; Macdiarmid, G. A.; Lelkes, I. P. *Biomaterials* **2006**, *27*, 2705.
- Zhou, X.; Cha, H.; Yang, C.; Zhang, W. *Anal. Chim. Acta* **1996**, *329*, 105.
- Yang, Y.; Mu, S. *J. Electroanal. Chem.* **1996**, *415*, 71.

4. Kwon, S. J.; Seo, M.; Yang, H.; Kim, S. Y.; Kwak, J. *Bull. Korean Chem. Soc.* **2010**, *31*, 3103.
  5. Yang, J.; Burkinshaw, M. S.; Zhou, J.; Monkman, P. A.; Brown, P. *J. Adv. Mater.* **2003**, *15*, 1081.
  6. Karg, S.; Scott, J. C.; Salem, J. R.; Angelopoulos, M. *Synth. Met.* **1996**, *80*, 111.
  7. Harlev, E.; Gulakhmedova, T.; Rubiniovich, I.; Aizenshtein, G. *Adv. Mater.* **1996**, *8*, 994.
  8. Chen, S. A.; Chuang, K. R.; Chao, C. I.; Lee, H. T. *Synth. Met.* **1996**, *82*, 207.
  9. Alam, M. M.; Wang, J.; Guo, Y.; Lee, P. S.; Tseng, R. H. *J. Phys. Chem. B* **2005**, *109*, 12777.
  10. Tseng, J. R.; Haung, J.; Ouyang, J.; Kaner, B. R.; Yang, Y. *Nano. Lett.* **2005**, *5*, 1077.
  11. Wang, J.; Chan, S.; Carlsoin, R. R.; Luo, Y.; Ge, G.; Ries, S. R.; Heath, R. J.; Tseng, R. H. *Nano. Lett.* **2004**, *4*, 1693.
  12. Ryu, K. S.; Kim, K. M.; Hong, Y. S.; Park, Y. J.; Chang, S. H. *Bull. Korean Chem. Soc.* **2002**, *23*, 1144.
  13. Roy, B. C.; Gupta, M. D.; Bhowmilk, L.; Ray, J. K. *Bull. Mater. Sci.* **2001**, *24*, 389.
  14. Iwuhoa, E. I.; Mavundla, S. E.; Somerset, V. S.; Petrik, L. F.; Klink, M. J.; Sekota, M.; Baker, P. *Microchim. Acta* **2006**, *155*, 453.
  15. Huang, J.; Kaner, R. B. *J. Am. Chem. Soc.* **2004**, *126*, 851.
  16. Sayyah, S. M.; Kamal, S. M.; Abd El-Rehim, S. S.; Ibrahim, M. A. *Int. J. Poly. Mater.* **2006**, *55*, 339.
  17. Norris, I. D.; Kane-Maguire, L. A. P.; Wallace, G. G. *Macromolecules* **2000**, *33*, 3237.
  18. Rivas, B. L.; Sanchez, C. O.; Bernede, J. C.; Mollinie, P. *Polymer Bulletin* **2002**, *49*, 257.
  19. Sayyah, S. M.; Azooz, R. E.; Abd El-Rehim, S. S.; El-Rabiey, M. *Int. J. Poly. Mater.* **2006**, *55*, 37.
  20. Huang, L.; Wen, T.; Gopalan, A. *Mater. Lett.* **2003**, *57*, 1765.
  21. Yan, H.; Wang, H. J.; Adisasmito, S.; Toshima, N. *Bull. Chem. Soc. Jpn.* **1996**, *69*, 2395.
  22. Chan, S. H.; Ng, C. S.; Sim, S. W.; Tan, L. K.; Tan, G. T. B. *Macromolecules* **1992**, *25*, 6029.
  23. Ghadimi, F.; Safa, K. D.; Massoumi, B.; Entezami, A. A. *Iran. Polym. J.* **2002**, *11*, 159.
  24. Penner, R. M.; Martin, C. R. *J. Electrochem. Soc.* **1986**, *133*, 310.
  25. Zhang, L.; Peng, H.; Fang, C.; Kilmartin, P. A.; Travas sejdic, J. *Nanotechnology* **2007**, *18*, 115607.
  26. Kunglin, H.; An chen, S. *Macromolecules* **2000**, *33*, 8117.
  27. Han, D.; Song, J.; Ding, X.; Xu, X.; Niu, L. *Mater. Chem. Phys.* **2007**, *105*, 380.
  28. Han, M. G.; Cho, S. K.; Oh, S. G.; Im, S. S. *Synth. Met.* **2002**, *126*, 53.
  29. Han, J.; Song, G.; Guo, R. *Adv. Mater.* **2006**, *18*, 3140.
  30. Luo, C.; Peng, H.; Zhang, L.; Lu, G. L.; Wang, Y.; Sejdic, J. T. *Macromolecules* **2011**, *44*, 6899.
  31. Laviron, E. *J. Electroanal. Chem.* **1974**, *52*, 355.
  32. Yang, G.; Tan, L.; Shi, Y.; Wang, S.; Lu, X.; Bai, H.; Yang, Y. *Bull. Korean Chem. Soc.* **2009**, *30*, 454.
  33. Wang, L.; Huang, P.; Bai, J.; Wang, H.; Wu, X.; Zhao, Y. *Int. J. Electrochem. Sci.* **2006**, *1*, 334.
  34. Wang, Y. *Microchim Acta* DOI 10.1007/s00604-010-0510-2
  35. Chang, J. L.; Chang, K. H.; Hu, C. C.; Cheng, W. L.; Zen, J. M., *Electrochem. Commun.* **2010**, *12*, 596.
  36. Wu, K.; Sun, Y.; Hu, S. *Sens. Actuators B* **2003**, *96*, 658.
  37. Tan, L.; Yang, G. M.; Wang, P.; Xie, Z. Y.; Bai, H. P.; Lu, X. X.; Yang, Y. H. *Anal. Lett.* **2008**, *41* 2860.
  38. Wang, S.; Lu, L.; Lin, X. *Electroanalysis* **2004**, *16*, 1734.
-